

# The Accretion of Gas onto Galaxies as Traced by their Satellites

Guinevere Kauffmann<sup>1</sup>, Cheng Li<sup>1</sup>, Timothy M. Heckman<sup>2</sup>,

<sup>1</sup>*Max-Planck Institut für Astrophysik, D-85748 Garching, Germany*

<sup>2</sup>*Department of Physics and Astronomy, Johns Hopkins University, Baltimore, MD 21218*

## Abstract

We have compiled a large sample of isolated central galaxies from the Sloan Digital Sky Survey, which do not have a neighbour of comparable brightness within a projected distance of 1 Mpc. We use the colours, luminosities and surface brightnesses of satellite galaxies in the vicinity of these objects to estimate their neutral gas content and to derive the average total mass of HI gas contained in the satellites as a function of projected radius from the primary. Recent calibrations of merging timescales from N-body simulations are used to estimate the rate at which this gas will accrete onto the central galaxies. Our estimated accretion rates fall short of those needed to maintain the observed level of star formation in these systems by nearly two orders of magnitude. Nevertheless, there are strong correlations between the total mass of gas in satellites and the colours and specific star formation rates of central galaxies of all stellar masses. The correlations are much weaker if we consider the total stellar mass in satellites, rather than their total gas mass. We ask *why* star formation in the central galaxies should be correlated with gas contained in satellites at projected separations of a Mpc or more, well outside the virial radius of the dark matter halos of these systems. We suggest that gas-rich satellites trace an underlying reservoir of ionized gas that is accreted continuously, and that provides the fuel for ongoing star formation in galaxies in the local Universe.

**Keywords:** galaxies: formation, evolution; galaxies: fundamental parameters; galaxies: haloes; galaxies: starbursts; galaxies: statistics; galaxies: stellar content; galaxies: structure

# 1 Introduction

Our current theoretical understanding of how galaxies form through the hierarchical formation of structure and through gas-dynamical dissipative processes (White & Rees 1978) leads to the view that star-forming spiral galaxies like our own Milky Way must continue to accrete gas at the present day. The observed size distribution of disk galaxies is consistent with models in which the specific angular momenta of the disks are similar to those of their present-day halos and in which the disks assemble recently ( $z < 1$  on average) (Mo, Mao & White 1998). The fraction of baryons in dark matter halos that have condensed into galaxies reaches a maximum of  $\sim 20\%$  at masses close to that of the Milky Way (Guo et al 2010). Unless the missing baryons have been ejected far from the halo by some catastrophic feedback mechanism, gas is predicted to accrete onto our Galaxy at the present epoch at average rates of around a few solar masses per year (e.g. Kauffmann, White & Guiderdoni 1993; De Lucia & Helmi 2008).

Observational support for continued accretion of gas in present-day disk galaxies comes from studies of their stellar populations, which indicate that star formation rates in the solar neighbourhood have remained fairly constant over much of the age of the Universe (Binney, Dehnen & Bertelli 2000). In addition, chemical evolution models of the Galaxy invoke continued gas infall and long formation timescales of the thin disk to explain chemical abundance ratios in disk stars (e.g. Chiappini, Matteucci & Gratton 1997). However, *direct* observational evidence for continued gas accretion remains elusive. In a recent review article, Sancisi et al (2008) provide a list of 24 nearby galaxies that appear to be interacting with companions with substantial HI gas. These authors estimate that around 25% of all spiral and irregular galaxies show evidence for such minor interactions. A very rough estimate of the resulting accretion rate is  $\sim 0.1 - 0.2 M_{\odot} \text{ yr}^{-1}$ , which is too low to maintain star formation in the Milky Way at its observed level of around  $2-3 M_{\odot} \text{ yr}^{-1}$ .

A similar argument that the main gas reservoir that fuels ongoing star formation in galaxies cannot be in the form of neutral hydrogen has been made in a paper by Hopkins et al (2008). These authors compare the cosmic evolution of the star formation rates in galaxies with that of their neutral hydrogen densities. Because the average star formation rates in galaxies drop steeply from high redshift to the present day, but the total neutral hydrogen density remains approximately constant with redshift, they conclude that HI must be continuously replenished from an external reservoir. This external reservoir may be in the form of a hot galactic corona in hydrostatic equilibrium with the surrounding dark matter halo. Thermal instabilities result in the formation of clouds of colder gas, which then rain onto the galactic disk (e.g. Peek, Putman & Sommer-Larsen 2008). Alternatively, the reservoir may reside in filaments formed during the non-linear collapse of structure predicted in CDM cosmologies (e.g. Keres et al 2005; Dekel et al 2009). In this case, one might expect galaxies containing significant neutral hydrogen to *trace* the underlying reservoir of ionized gas, because these galaxies would be located in the higher density collapsed halos that make up the filaments.

A statistical analysis of how the properties of companion (or satellite) galaxies relate to the properties of their hosts is only possible using large optical imaging and spectroscopic surveys such as the Sloan Digital Sky Survey (SDSS; York et al. 2000) or the Two Degree Field Survey (2dF; Colless et al 2001). Traditionally, the average number density profiles and line-of-sight velocity dispersions of satellites are used to place constraints on the density profiles of the dark matter halos surrounding their hosts (Zaritsky & White 1994; Prada et al 2003). A few studies have examined whether there are correlations between satellites and hosts in terms of directly observable quantities such as colour or morphological type. In particular, Weinmann et al (2006) found that the fraction of early-type satellites is significantly higher in a halo with an early-type central galaxy than in a halo of the same mass with a late-type central galaxy. They dubbed this phenomenon “galactic

conformity”, but did not come up with a compelling explanation for why it should occur.

In this paper, we revisit the connection between satellite galaxies and their hosts. We use the colour, luminosity and surface brightness of each satellite to estimate both its stellar mass and its neutral gas fraction using empirical relations from the literature. We stack together host galaxies with similar properties (such as stellar mass and colour) and compute the total stellar and gas mass contained in satellites as a function of projected radius  $R_p$ . Finally, we study how these average stellar and gas mass profiles depend on the properties of the host, and we argue that the “galactic conformity” phenomenon can be understood in terms of ongoing fuelling of the interstellar medium of galaxies by a reservoir of gas that is associated with their satellites.

Our paper is organized as follows. In section 2, we describe the spectroscopic and photometric galaxy samples used in our analysis, as well as our methodology for calculating the average radial profiles of the total stellar and gas mass contained in satellites. In section 3, we present the radial profiles as a function of the stellar mass of the host and we confirm that the total amount of neutral gas contained in the satellites falls far short of what is needed to maintain the observed levels of star formation in the hosts. In section 4, we examine correlations between the total amount of neutral gas and stellar mass in the satellites and properties of the hosts, such as colour, concentration index and stellar surface mass density. We demonstrate that the primary correlation is between the total amount of gas in the satellites and the stellar populations of the hosts. In section 5, we present what we believe to be the most likely interpretation of our results. We assume a  $\Lambda$ CDM cosmology with  $\Omega_m=0.3$ ,  $\Omega_\Lambda = 0.7$  and  $h = 0.7$  throughout.

## 2 The Data

### 2.1 The Photometric Sample of Satellites

Our sample is constructed using the “datasweep” files included as part of the New York University Value Added Catalogue (NYU-VAGC; Blanton et al. 2005). This is a compressed version of the full photometric catalogue of the SDSS Data Release 7 (Abazajian et al. 2009) that was used by Blanton et al. to build the NYU-VAGC. The reader is referred to Blanton et al. (2005) for a detailed description of the NYU-VAGC. More information about the datasweep files is also available at <http://sdss.physics.nyu.edu/vagc/>. There are two catalogues in the datasweep, one for stars and one for galaxies. Starting from the galaxy catalogue, we select all galaxies with  $r$ -band apparent model magnitudes in the range  $10 < r < 21$  after correction for Galactic extinction, and PSF and model magnitudes satisfying  $m_{psf} - m_{model} > 0.145$  in all five bands. In order to select unique objects in a run that are not at the edge of field, we require the RUN PRIMARY flag to be set, and the RUN EDGE flag not to be set. This procedure results in a final sample of  $\sim 26$  million galaxies.

### 2.2 The Spectroscopic Sample of Primaries

The parent sample of primary galaxies for this study is composed of 397,344 objects which have been spectroscopically confirmed as galaxies and have data publicly available in the SDSS Data Release 4 (Adelman-McCarthy et al 2006). These galaxies are part of the SDSS main galaxy sample used for large scale structure studies (Strauss et al 2002) and have Petrosian  $r$  magnitudes in the range  $14.5 < r < 17.77$  after correction for foreground galactic extinction using the reddening maps of Schlegel, Finkbeiner & Davis (1998). Their redshift distribution extends from 0.005 to 0.30, with a median redshift of 0.10. Stellar masses, metallicity and star formation rate estimates, as well as spectral indices such as the 4000 Å break strengths are available at <http://www.mpa-garching.mpg.de/SDSS/DR4/> (see Kauffmann et al 2003; Brinchmann et al 2004; Tremonti et al

2004 for more details). In this analysis we, further limit the spectroscopic sample to galaxies with  $r < 17$ , so that we are able to probe satellites down to a limiting magnitude that is 4 magnitudes fainter than the primary (i.e. roughly a factor 40 smaller in stellar mass). We also restrict the sample to lie at redshifts  $z > 0.03$ , so that we are able to probe satellites to reasonably large projected radii from the primary object. Finally, we eliminate galaxies that lie at projected radii of less than 1 Mpc from the photometric survey boundaries.

### 2.3 Estimating the Stellar and Gas Masses of the Satellites

We begin by finding all galaxies in the photometric sample that lie within 1 Mpc in projected radius from the primary. The projected radius is calculated by placing the satellite at the same redshift as the primary ( $z_{prim}$ ). Some galaxies will be interlopers that are actually at a very different redshift, but we will correct the stellar and gas mass profiles for this effect via statistical background subtraction.

The next step is to estimate k-corrections and stellar  $M/L$  ratios for the satellites. Following the procedure outlined in Bell et al (2003), we compare the  $gri$  fluxes of the galaxies with a set of stellar population synthesis (SPS) models (we do not use the  $u$  or  $z$  band fluxes, because they have much larger errors). Bruzual & Charlot (2003) stellar population synthesis models are used to construct a set of models in which the star formation histories vary exponentially with time and we tabulate the observed  $g - r$  and  $r - i$  colours of each model at a set of different redshifts (0.03 to 0.3, in  $\Delta z$  bins of 0.01). If the colours of the satellites lie outside the range of colours predicted by the model at  $z = z_{prim}$ , then the satellite is discarded from the analysis. In practice, this procedure eliminates a large fraction of the reddest galaxies with  $r - i$  colours that imply that they must lie at high redshifts (Collister et al. 2007), and significantly improves the  $S/N$  of our mass profiles. For the galaxies that remain, we use the best-fit model to derive k-corrected colours at  $z = 0$ . These colours are then used to estimate the stellar mass-to-light-ratio using the formula  $\log(M/L)_i = -0.222 + 0.864(g - r)_{(z=0)} - 0.15$  given in Table 7 of Bell et al (2003) for a Kroupa IMF. As discussed in Bell et al (2003), typical  $M/L$  ratio uncertainties are expected to be  $\sim 0.1$  dex.

In a recent paper, Zhang et al. (2009) used a sample of 800 galaxies with HI mass measurements from the HyperLeda catalogue and optical photometry from SDSS to calibrate a new photometric estimator of the HI-to-stellar-mass ratio for nearby galaxies. The estimator is  $\log(GHI/S) = -1.73238(g - r)_{(z=0)} + 0.215182\mu_i - 4.08451$ , where  $\mu_i$  is the i-band surface brightness estimated within the half-light radius of the galaxy. The estimator was shown to have a scatter of 0.31 dex in  $\log(GHI/S)$ . The authors did not find any significant dependence of the residuals on galaxy properties such as stellar mass or mean stellar age (as measured by the 4000Å break strength). In this paper, we use this estimator to calculate an HI mass for each of our satellite galaxies.

### 2.4 Correction for interlopers

We have generated 20 catalogs of galaxies that are spread over the same area of sky as our sample of primary galaxies, but with randomly generated sky coordinates. The galaxies in the random catalogues are assigned the redshifts and IDs of the galaxies in our primary sample, and we proceed to find “satellites” in the photometric catalogue in exactly the same way as for the real sample of primaries. We also apply exactly the same procedures to derive k-corrections, to throw out galaxies that do not fit in the predicted colour range, and to derive stellar and gas masses. This allows us to estimate what fraction of the stellar mass and gas mass at radius  $R_p$  originates from interlopers, rather than from true, physically-associated satellite systems.

Because the contamination by interlopers at a given value of  $R_p$  in physical units will depend on the redshift of the primary galaxy, it is important to compute the back ground using random galaxies with exactly the same distribution of redshifts as that of the real primary galaxies in our stacks. Our procedure, therefore, can be summarized as follows:

1. Partition the sample of primary galaxies into bins of a given property (e.g. stellar mass).
2. Find satellites within 1 Mpc of each primary and estimate stellar and gas masses.
3. Compute the average stellar and HI mass profiles as a function of projected radius for the sum of all primaries in given bin.
4. Repeat steps 2 and 3 above for the corresponding set of randomly distributed primaries.
5. The final stellar mass or HI mass profile for galaxies in a given bin is found by subtracting the average profiles obtained for the randomly distributed primaries from the profiles derived in step 3 above.

## 3 Results

### 3.1 Stellar and Gas Mass Profiles

In Figure 1, we show plots of the cumulative stellar and gas mass contained in satellites interior to a projected radius  $R_p$ . Results are shown in bins of stellar mass. The red curves show the integrated stellar mass profiles, while the blue curves show the integrated HI gas mass profiles. To guide the eye, we re-plot the curves in the first panel using dotted blue and red line styles.

As can be seen, the total stellar mass contained in satellites increases as a function of the stellar mass of the primary. This increase is seen at all value of  $R_p$ . However, the total mass of gas contained in satellites exhibits quite different behaviour as a function of the stellar mass of the primary galaxy. On small scales, the mass in gas actually *decreases* as a function of increasing host galaxy mass.

One problem with simply stacking together all galaxies in bins of stellar mass, is that one is effectively averaging together galaxies in many different environments. In particular, a galaxy with a stellar mass of a few  $\times 10^{10} M_\odot$  could be a central galaxy in a halo of mass  $\sim 10^{12} M_\odot$ , or it could be a satellite galaxy in a much larger halo, with mass corresponding to that of a group or cluster. Satellite galaxies in groups or clusters are known to have redder colours and lower star formation rates than their counterparts in low density environments. It is hypothesized that the main reason for this is that the external gas reservoirs of satellites are stripped as they orbit within the cluster potential. Because the main goal of this study is to understand if there is a link between star formation in a galaxy and the gas contained in satellites, it is important to remove primary galaxies that are themselves satellite systems in massive dark matter halos.

We do this by imposing an isolation criterion on our sample of primaries. We exclude all galaxies with a neighbour with an apparent magnitude brighter than  $r_{prim} + 0.4$  mag (where  $r_{prim}$  is the r-band model magnitude of the primary) within a projected radius of 1 Mpc from the primary. This is a fairly stringent criterion that should eliminate all galaxies located in groups and clusters.<sup>1</sup> The stellar mass and gas mass profiles of this sample of isolated primaries is shown in Figure 2. We overplot the mass profiles for the full samples as dashed lines in order to show the effect of the isolation criterion. As can be seen, the cut has the largest effect on the low mass primaries. For

---

<sup>1</sup>Note that we have experimented with different isolation criteria, and none of our conclusions would change if we adopted a different cut.

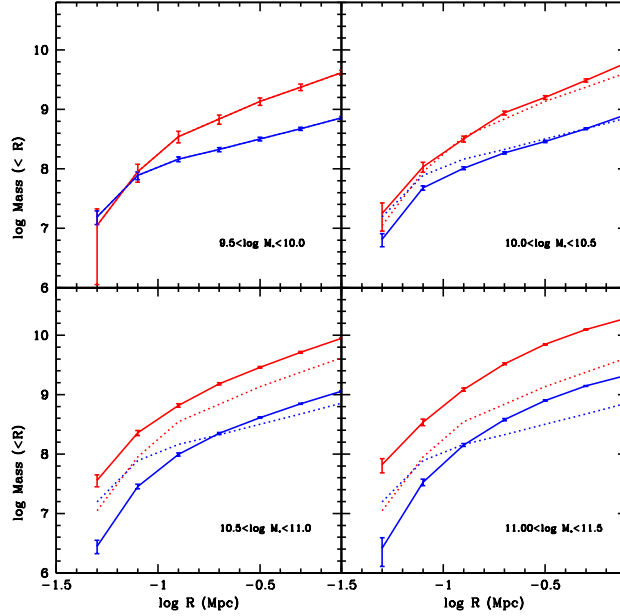


Figure 1: Cumulative stellar (red) and gas mass (blue) contained in satellites interior to projected radius  $R_p$ . Results are shown in four different bins of stellar mass. The dotted lines are plotted to guide the eye and simply repeat the profiles in the first panel.

galaxies with stellar masses less than a few  $\times 10^{10} M_\odot$ , the stellar mass contained within a projected radius of 1 Mpc drops by an order of magnitude, showing that most of the contribution is coming from massive halos. On the other hand, the gas mass within 1 Mpc drops by less than a factor of two, presumably because most of the galaxies in massive halos are red systems with small HI fractions. For galaxies with stellar masses greater than  $10^{11} M_\odot$ , the isolation criterion has very little effect, because most of these galaxies are the central galaxies of their halo. We have also marked the expected location of the virial radius of the dark matter halos of the galaxies in each stellar mass bin. We adopt the standard definition of the virial radius as the radius within which the dark matter over-density is 200 times the critical density, and we use the empirically-calibrated relation between the stellar mass of a central galaxy and its dark matter halo mass given in Table 2 of Wang et al (2006).

### 3.2 The inferred gas accretion rate

We now estimate the average rate at which gas contained in satellites will accrete onto central galaxies as a function of their mass, and compare the estimated gas accretion rate with the average star formation rates in the primaries. To do this, we make use of the calibration between the projected separation of a pair of galaxies and the average time until the merger given in Kitzbichler & White (2008). These authors use virtual galaxy catalogues derived from the Millennium Simulation (Springel et al 2005) to derive sample-averaged merging times as a function of projected separation, the stellar masses of the galaxies in the pair, and redshift. At  $z < 2$ , the timescale  $T$  is only weakly dependent on mass and can be approximated as  $T \sim T_0 r_{25} M_*^{-0.3}$ , where  $r_{25}$  is the projected separation in units of  $25 h^{-1}$  kpc and the coefficient  $T_0$  is 1.6 Gyr (appropriate for samples where the line-of-sight velocity difference between the two galaxies is unconstrained).

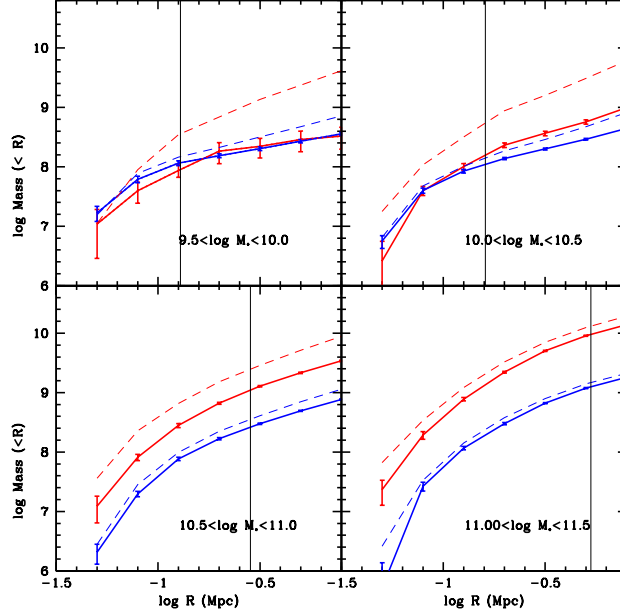


Figure 2: Cumulative stellar (red) and gas mass (blue) contained in satellites interior to projected radius  $R_p$  around “central” galaxies (see text). The dashed lines show the results obtained for all galaxies, as plotted in Figure 1. The vertical black lines show the expected location of the virial radius of a dark matter halo hosting a galaxy in the given stellar mass range (see text).

In the left panel of Figure 3, we plot the average star formation rates of the central galaxies in our sample for 5 different bins in stellar mass. The star formation rates are estimated using emission line fluxes and ratios measured from the SDSS spectra and corrected for aperture effects as described in Brinchmann et al (2004). The star formation rates rise from  $\sim 1.5 M_\odot \text{ yr}^{-1}$  for central galaxies of  $10^9 M_\odot$  to  $\sim 3 M_\odot \text{ yr}^{-1}$  for central galaxies like the Milky Way with stellar masses of  $3 \times 10^{10} - 10^{11} M_\odot$ . In the middle panel, we plot the merging time as a function of projected radius  $R_p$  given by the calibration of Kitzbichler & White (2008). Blue, green, black, red and magenta lines show results for the five mass bins plotted in the left panel, with stellar mass increasing as colour goes from blue to magenta. Finally, in the right panel we plot the fraction of the total star formation rate of the primary galaxy that is contributed from gas accretion in satellites interior to radius  $R_p$ , i.e.  $M_{\text{gas}}(r < R_p)/T(R_p)/SFR_{\text{primary}}$ .

It is interesting that for low mass primaries, the curves are reasonably flat, so it does not matter what radius one adopts to estimate the gas accretion rate. For high mass primaries, the estimated accretion rate drops at small projected separations. It is reasonable that not all the gas present in a satellite far from the primary will remain available to fuel star formation by the time that satellite has finally reached the centre of the halo. Part of the gas may be consumed into stars or stripped out of the galaxy. However, we caution against drawing too many strong conclusions about satellite stripping processes from these result. The merging times calibrated by Kitzbichler & White are not guaranteed to remain accurate at very small pair separations, because the resolution of the Millennium Simulation was not high enough to track the orbital evolution of merging galaxies in detail. The main conclusion from Figure 3 is that the estimated gas accretion rates from satellites always fall short of what is needed to maintain the observed level of star formation in the primary

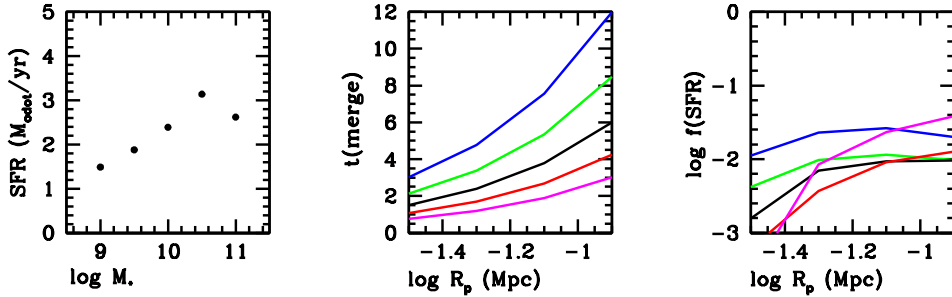


Figure 3: *Left*: Average star formation rates of the central galaxies in our sample for 5 different bins in stellar mass. *Middle*: Merging time as a function of projected radius  $R_p$  as given by the calibration of Kitzbichler & White (2008). Blue, green, black, red and magenta lines show results for the five mass bins plotted in the left panel, with stellar mass increasing from blue to magenta. *Right*: The fraction of the total star formation rate of the primary galaxy that is contributed from accreted gas in satellites interior to radius  $R_p$ .

galaxies by around two orders of magnitude. This shortfall is roughly independent of the mass of the primary.

## 4 Correlations with properties of the primaries

In this section we examine whether the integrated stellar mass and gas mass profiles of satellites correlate with the properties of the primary. In Figure 4, we split the our primary sample into “blue sequence” galaxies with  $g-r < 0.65$  and “red sequence” galaxies with  $g-r > 0.65$ <sup>2</sup> and we plot the stellar and gas mass profiles for four different bins in the stellar mass of the primary. Interestingly, the stellar mass profiles of the satellites do not correlate with the colours of the central galaxies, but there is significantly more gas present in the satellites around the blue central galaxies. The effect is strongest at small radii, but persists out to projected distances of  $\sim 1$ , except in our highest stellar mass bin. Note that the fraction of blue central galaxies is a very strong function of stellar mass. In the lowest mass bin ( $9.5 < \log M_* < 10$ ), there are too few red galaxies to include in the plot, and in our highest mass bin ( $11.0 < \log M_* < 11.5$ ), blue galaxies comprise only a few percent of the sample. Nevertheless, the strong systematic difference in the gas profiles around red and blue galaxies is present at all stellar masses.

Figure 5 expands upon these results by showing what happens if we further divide galaxies by colour. The thick red and blue curves repeat the results shown in Figure 4. The green and cyan curves are for galaxies with  $g-r < 0.45$  and  $g-r < 0.35$ , respectively. The magenta curves are for galaxies with  $g-r > 0.75$ . As can be seen, the colours of red sequence galaxies do not appear to be related to either the stellar mass or the gas mass profiles of the satellites in their vicinity. However, on the blue sequence there is a clear and monotonic trend for the amount of gas to increase as the colour of the primary becomes bluer. For the bluest primaries, one also sees an increase in the stellar mass contained in satellites, but the effect is weaker than that seen for the gas. An increase in the *number* of satellites around the most strongly star-forming galaxies is to be expected. Previous work has

<sup>2</sup>Note that the division between the red and blue sequence moves to slightly redder colours at higher stellar masses, but for simplicity we choose a fixed cut in colour



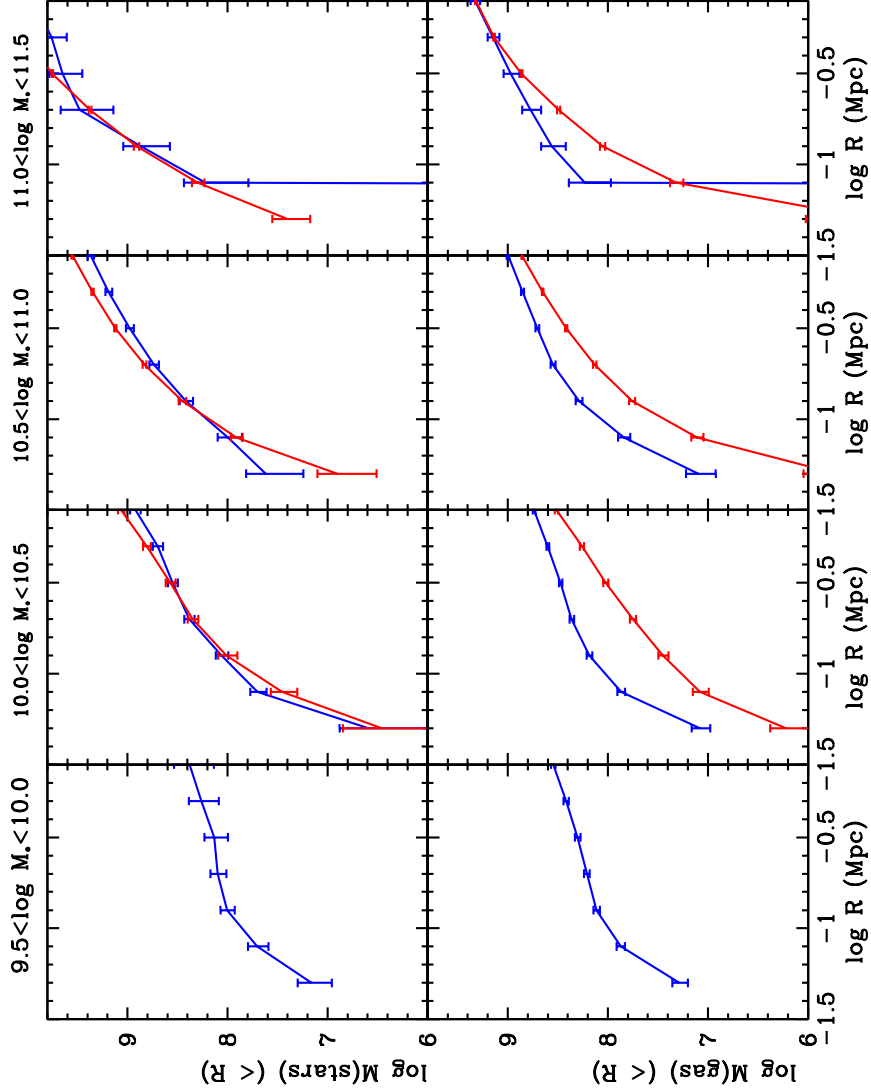


Figure 4: Cumulative stellar (top) and gas mass (bottom) contained in satellites interior to projected radius  $R_p$  around “central” galaxies. The central galaxy population is divided into blue sequence galaxies with  $g - r < 0.65$  (blue curves) and red sequence galaxies with  $g - r > 0.65$  (red curves).

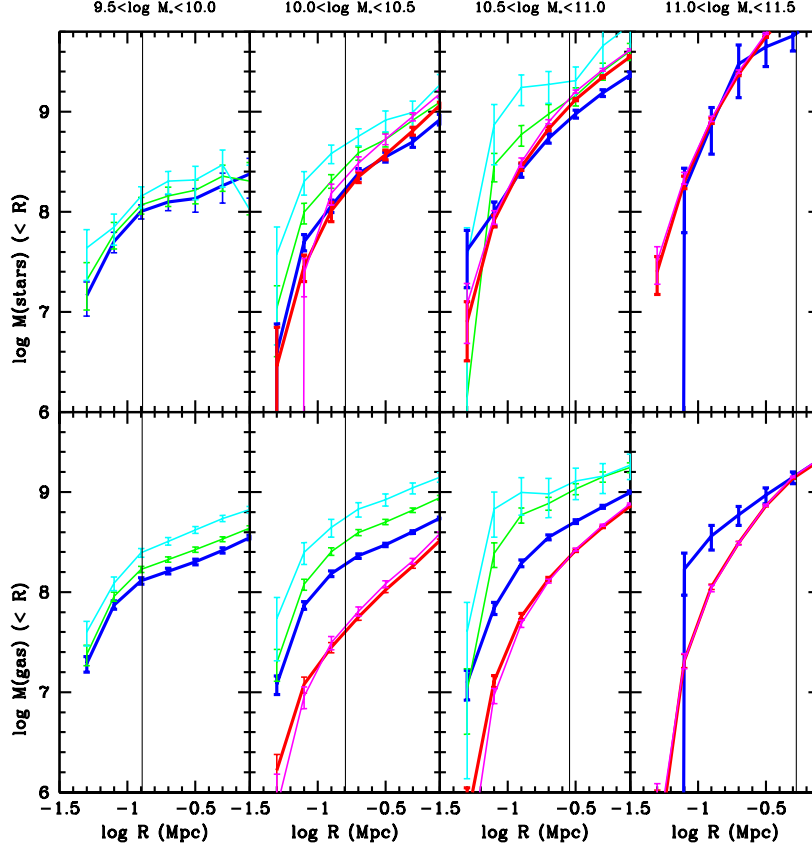


Figure 5: Cumulative stellar (top) and gas mass (bottom) contained in satellites interior to projected radius  $R_p$  around “central” galaxies. The central galaxy population is divided into blue sequence galaxies with  $g-r < 0.65$  (blue curves) and red sequence galaxies with  $g-r > 0.65$  (red curves). In addition, the blue sequence is further subdivided into galaxies with  $g-r < 0.45$  (green) and  $g-r < 0.35$  (cyan). Magenta curves show the very reddest galaxies with  $g-r > 0.75$ . The vertical black lines show the expected location of the virial radius of the dark matter halos that host galaxies in the given stellar mass range.

shown that that most strongly star-forming galaxies exhibit an excess of close pairs (Barton, Geller & Kenyon 2000; Li et al 2008), and this is generally understood as evidence that tidal interactions between galaxies induce higher rates of star formation in these objects. What is surprising about our results, is that if one re-expresses the traditional statistics of close pairs in terms of the *gas content* of the nearby satellites, the trends become much stronger and also extend over the whole blue sequence, instead of just being apparent for the most strongly star-bursting galaxies. We will come back to this point in the discussion.

Finally, we note that the correlation between the colour of the primary and the gas contained in satellites is not a phenomenon confined to satellites at small spatial separations from the primary ; Figure 5 shows the correlation persists beyond scales of  $\sim 1$  Mpc, i.e. beyond the virial radius of the dark matter halo for the majority of the primaries in our sample. Only for the the most massive primaries with stellar masses  $\sim 10^{11} M_\odot$ , is there some evidence that the correlation is confined to satellites within the virial radius of the dark matter halo.

## 4.1 Star formation or morphology?

The results discussed above have been presented in the literature before, albeit in a different form. Weinmann et al (2006) studied correlations between the properties of satellites and central galaxies using data from the Sloan Digital Sky Survey Data Release 2. They found that the "early-type" fraction of satellite galaxies is significantly higher in a halo with an early-type central galaxy, than in a halo of the same mass with a late-type central galaxy. They dubbed this phenomenon 'galactic conformity' and considered a variety of processes that might give rise to the effect, including mergers, harassment in clusters and ram-pressure stripping, but concluded that none of these could provide a compelling explanation for the observational trends.

We note that the physical processes discussed in the Weinmann et al paper are ones that would alter the *structural* properties of the galaxies, but in actual fact colours and spectral indices such as the 4000 Å break strength were used to classify the galaxies in the sample by type. It is well known that the star formation rates in galaxies correlate strongly with their structural properties. Galaxies with low stellar masses, stellar surface densities and concentrations tend to be blue, while galaxies with high masses, stellar surface densities and concentrations, tend to be red. This is why spectral type and galaxy structure are frequently lumped together under the general term "morphology". If one wishes to understand whether a given physical process (e.g. gas accretion) could be responsible for the correlation between the properties of central galaxies and their satellites, it is very important to decouple the star formation/galaxy structure link and understand which of the two properties is *primarily* affected by the phenomenon under consideration.

Our attempt to do this is shown in Figure 6. We plot contours of the total gas mass in satellites estimated within a fixed aperture of  $R_p = 300$  kpc. We show our results in the two-dimensional plane of  $g - r$  colour versus stellar surface mass density  $\mu_*$  and concentration index (Concentration index  $C$  is defined as the ratio between the radius enclosing 90% of the total Petrosian flux of the galaxy in the  $r$ -band and the radius enclosing 50% of this flux <sup>3</sup>) Results are shown for two different bins in stellar mass. As can be seen, there is a strong correlation between central galaxy colour and both surface density and concentration, so that galaxies in our sample only occupy a relatively narrow strip in the plots. We can also see that the contours of constant gas mass in satellites always run parallel to the x-axis in all four panels, showing that the main link is between gas mass in satellites and the colour of the central galaxy, and not between gas mass and the structure of the central galaxy.

## 5 Discussion

We now discuss the main conclusions and implications of this work.

**1. The cold gas contained in satellites is not sufficient to provide the fuel for ongoing star formation in central galaxies.** As discussed in the introduction, this conclusion is not a surprise. We note that our estimate of the accretion rate from gas in satellites is a factor of 2-5 lower than that of Sancisi et al (2008). There are two likely reasons for this: a) we use merging timescales from Kitzbichler & White (2008), which are a factor of 2 longer than most other published determinations of merger rates, b) the Sancisi et al study focuses on galaxies with significant HI content, whereas our study averages over all galaxies of a given stellar mass. As we have demonstrated, there is a strong *correlation* between the colours (and hence gas content) of central galaxies and the mass of gas in their satellites in the sense that bluer and more gas-rich galaxies should have more gas in

---

<sup>3</sup>As shown in Figure 1 of Weinmann et al (2009), the concentration index correlates very well with the bulge-to-disk ratios obtained by 2-dimensional multi-component fits of Gadotti (2008) using the BUDDA code.

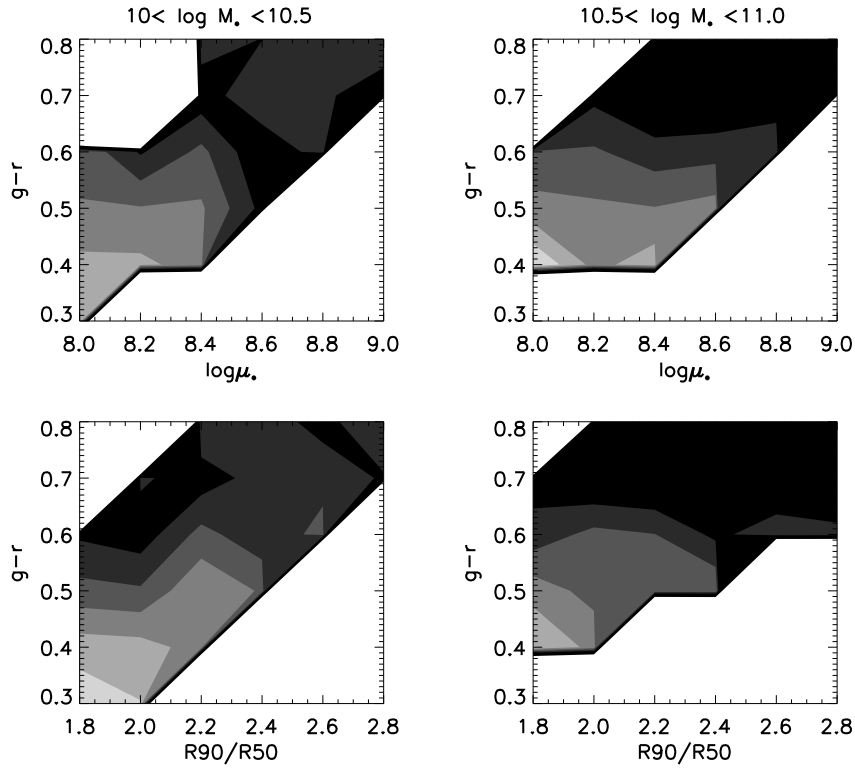


Figure 6: Contours of the total gas mass in satellites estimated within a fixed aperture of  $R_p = 300$  kpc. We show the results in the plane of  $g - r$  colour versus stellar surface mass density  $\mu_*$  and concentration index, defined as the ratio between the radius enclosing 90% of the total Petrosian flux of the galaxy in the  $r$ -band and the radius enclosing 50% of this flux.

satellites in their immediate surroundings.

**2. Star formation in central galaxies is strongly correlated with the mass of gas contained in the satellites** It is not easy to understand *why* the properties of central and satellite galaxies that are separated by distances of hundreds of kiloparsecs to several Mpc ought to correlate. One explanation that should be considered is that it is the central galaxy that somehow affects the properties of its satellites. Weinmann et al (2006) and Ann, Park & Choi (2008) argue that the satellites of early-type central galaxies are likely to be deprived of their gas reservoirs through hydrodynamic interactions with the X-ray emitting hot gas of their host.

We do not think this is a viable explanation of our results, because we have shown that the correlation between star formation in the host and gas in the satellites extends down to central galaxies with stellar masses of a few  $\times 10^9 M_\odot$ . These galaxies are not massive enough to have hot gas halos. In addition, the correlations are only present for galaxies on the blue sequence; there is no apparent relation between the colours of galaxies on the red sequence and the gas contained in their satellites.

The hypothesis that we deem more likely is that the satellites *trace a much larger underlying reservoir of ionized gas* that is accreting onto the central galaxies in a roughly continuous fashion. N-body plus hydrodynamical simulations of structure formation assuming a standard  $\Lambda$ CDM cosmology show that baryons in the  $z = 0$  universe are partitioned relatively evenly between a condensed phase consisting of stars and cold galactic gas, a diffuse phase consisting of photo-ionized intergalactic gas with temperatures below  $10^5$  K, and the so-called warm-hot intergalactic medium (WHIM) consisting of collisionally ionized gas at temperatures of between  $10^5$  and  $10^7$  K (e.g. Cen & Ostriker 1999; Dave et al 2001; Kang et al 2005). Most of the WHIM gas is too diffuse to self-gravitate or self-shield, and thus cannot achieve the densities required to make radiative cooling processes important (Dave et al 2001). Detailed studies of gas accretion onto galaxies with hydrodynamical simulations show that much of the gas reservoir for star formation is in the form of  $10^4 - 10^6$  K gas associated with filaments with coherence length of greater than 1 Mpc (Keres et al 2009).

These studies then suggest that the satellite galaxies analyzed in this paper trace the high density peaks of an underlying cosmic web of mostly photo-ionized gas at reasonably high overdensities, and that this ionized gas is the primary reservoir for future star formation in the galaxy. If there is more gas in satellites in the vicinity of a given galaxy, there is also likely to be more diffuse gas between the satellites. This would explain why there are such strong correlations between star formation and cold gas in satellites that are at distances of a Megaparsec or more from the primary, where infall times are long and the gas in the satellites themselves could never have had any physical contact with the primary galaxy.

**3. The same correlation is seen for galaxies with stellar masses greater than  $10^{11} M_\odot$ .** Mandelbaum et al (2006) have determined the average relation between the stellar mass of a galaxy and the mass of its dark matter halo from an analysis of galaxy-galaxy weak lensing in the SDSS. Late-type galaxies with masses of  $10^{11} M_\odot$  were found to reside in dark matter halos of mass  $\sim 2 \times 10^{12} M_\odot$ , while early-type galaxies of the same stellar mass were located in somewhat more massive halos ( $\sim 5 \times 10^{12} M_\odot$ ). Hydrodynamical simulations show that atmospheres of hot virialized gas develop in halos more massive than  $2 - 3 \times 10^{11} M_\odot$  and this transition mass remains nearly constant with redshift (e.g. Keres et al 2005, 2009).

One important question is whether star formation in the most massive galaxies is fuelled by gas that accretes from the hot phase. Models have been proposed (Maller & Bullock 2004; Kaufmann et al 2006; Peek, Putman & Sommer-Larsen 2008) in which ongoing accretion onto galactic disks progresses via the unstable cooling of the baryonic halo into condensed clouds, which then rain onto the disk. If this is the main mode by which gas reaches central galaxies in massive halos, one would

no longer expect to see any correlation between star formation in these objects and the amount of gas contained in satellites. The fact that the correlation persists for the most massive galaxies in our sample supports the hypothesis that blue massive galaxies are found in a *small subset* of halos where the gas reservoir is still spatially linked to satellite galaxies with neutral gas. The reason why blue massive galaxies are rare is because the majority of massive halos have completely transitioned to supporting hot gas atmospheres, which are unable to cool efficiently and form stars

Although we believe that the picture put forward in this concluding discussion is a plausible one, detection of the underlying reservoir will be required before we can be sure that we have located the fuel supply for ongoing star formation in nearby galaxies. Unfortunately the temperature and low density of diffuse gas around galaxies leave it nearly undetectable in emission. The most direct evidence we have that this component exists comes from studies of higher ionization lines of oxygen detected in absorption against background quasars (e.g. Richter et al 2004). These observations only probe individual sightlines and cannot accurately map the distribution and extent of the cosmic web. Nevertheless, if one has available a large enough sample of sightlines that pass within a few Mpc of nearby galaxies, one might nevertheless expect to see strong statistical correlations between star formation in the galaxy and the inferred column density of warm hydrogen, similar to the correlation we have found between star formation and the total gas contained in satellites. This may be possible in future with the Cosmic Origins Spectrograph (COS) on board the Hubble Space Telescope. Eventually, imaging of the IGM through its emission in Ly $\alpha$  may become possible with a wide-field UV spectral imaging telescope in space (Sembach et al 2009), or with next generation X-ray observatories that will be able to detect higher temperature gas (Bregman et al 2009).

## Acknowledgements

Funding for the creation and distribution of the SDSS Archive has been provided by the Alfred P. Sloan Foundation, the Participating Institutions, the National Aeronautics and Space Administration, the National Science Foundation, the U.S. Department of Energy, the Japanese Monbukagakusho, and the Max Planck Society. The SDSS Web site is <http://www.sdss.org/>. The SDSS is managed by the Astrophysical Research Consortium (ARC) for the Participating Institutions. The Participating Institutions are The University of Chicago, Fermilab, the Institute for Advanced Study, the Japan Participation Group, The Johns Hopkins University, the Korean Scientist Group, Los Alamos National Laboratory, the Max-Planck-Institute for Astronomy (MPIA), the Max-Planck-Institute for Astrophysics (MPA), New Mexico State University, University of Pittsburgh, University of Portsmouth, Princeton University, the United States Naval Observatory, and the University of Washington.

## References

- Abazajian K. N., et al., 2009, *ApJS*, 182, 543
- Adelman-McCarthy J. K., et al., 2006, *ApJS*, 162, 38
- Ann H. B., Park C., Choi Y.-Y., 2008, *MNRAS*, 389, 86
- Barton E. J., Geller M. J., Kenyon S. J., 2000, *ApJ*, 530, 660
- Bell E. F., McIntosh D. H., Katz N., Weinberg M. D., 2003, *ApJS*, 149, 289
- Blanton M. R., et al., 2005, *AJ*, 129, 2562
- Binney J., Dehnen W., Bertelli G., 2000, *MNRAS*, 318, 658
- Bregman J. N., et al., 2009, *astro*, 2010, 24
- Brinchmann J., Charlot S., White S. D. M., Tremonti C., Kauffmann G., Heckman T., Brinkmann J., 2004, *MNRAS*, 351, 1151
- Bruzual G., Charlot S., 2003, *MNRAS*, 344, 1000
- Cen R., Ostriker J. P., 1999, *ApJ*, 514, 1
- Chiappini C., Matteucci F., Gratton R., 1997, *ApJ*, 477, 765
- Colless M., et al., 2001, *MNRAS*, 328, 1039
- Collister A., et al., 2007, *MNRAS*, 375, 68
- Davé R., et al., 2001, *ApJ*, 552, 473
- De Lucia G., Helmi A., 2008, *MNRAS*, 391, 14
- Dekel A., et al., 2009, *Natur*, 457, 451
- Gadotti D. A., 2008, *MNRAS*, 384, 420
- Guo Q., White S., Li C., Boylan-Kolchin M., 2010, *MNRAS*, 367
- Hopkins A. M., McClure-Griffiths N. M., Gaensler B. M., 2008, *ApJ*, 682, L13
- Kang H., Ryu D., Cen R., Song D., 2005, *ApJ*, 620, 21
- Kauffmann G., White S. D. M., Guiderdoni B., 1993, *MNRAS*, 264, 201
- Kauffmann G., et al., 2003, *MNRAS*, 346, 1055
- Kaufmann T., Mayer L., Wadsley J., Stadel J., Moore B., 2006, *MNRAS*, 370, 1612
- Kereš D., Katz N., Weinberg D. H., Davé R., 2005, *MNRAS*, 363, 2
- Kereš D., Katz N., Davé R., Fardal M., Weinberg D. H., 2009, *MNRAS*, 396, 2332
- Kitzbichler M. G., White S. D. M., 2007, *MNRAS*, 376, 2

Li, C., Kauffmann G., Heckman T. M., Jing Y. P., White S. D. M., 2008, MNRAS, 385, 1903

Maller A. H., Bullock J. S., 2004, MNRAS, 355, 694

Mandelbaum R., Seljak U., Kauffmann G., Hirata C. M., Brinkmann J., 2006, MNRAS, 368, 715

Mo H. J., Mao S., White S. D. M., 1998, MNRAS, 295, 319

Peek J. E. G., Putman M. E., Sommer-Larsen J., 2008, ApJ, 674, 227

Prada F., et al., 2003, ApJ, 598, 260

Richter P., Savage B. D., Tripp T. M., Sembach K. R., 2004, ApJS, 153, 165

Sancisi R., Fraternali F., Oosterloo T., van der Hulst T., 2008, A&ARv, 15, 189

Schlegel D. J., Finkbeiner D. P., Davis M., 1998, ApJ, 500, 525

Sembach K., et al., 2009, astro, 2010, 54

Springel V., et al., 2005, Natur, 435, 629

Strauss M. A., et al., 2002, AJ, 124, 1810

Tremonti C. A., et al., 2004, ApJ, 613, 898

Wang L., Li C., Kauffmann G., De Lucia G., 2006, MNRAS, 371, 537

Weinmann S. M., van den Bosch F. C., Yang X., Mo H. J., 2006, MNRAS, 366, 2

White S. D. M., Rees M. J., 1978, MNRAS, 183, 341

York D. G., et al., 2000, AJ, 120, 1579

Zaritsky D., White S. D. M., 1994, ApJ, 435, 599

Zhang W., Li C., Kauffmann G., Zou H., Catinella B., Shen S., Guo Q., Chang R., 2009, MNRAS, 397, 1243